the FEBS Journal

Immunonanoparticles – an effective tool to impair harmful proteolysis in invasive breast tumor cells

Nataša Obermajer[1], Petra Kocbek[1], Urška Repnik[2], Alenka Kužnik[1], Mateja Cegnar[1], Julijana Kristl[1] and Janko Kos[1,2]

1 Faculty of Pharmacy, University of Ljubljana, Slovenia
2 Institute Jozef Stefan, Jamova Ljubljana, Slovenia

Keywords
antibody-coated; breast cancer; cystatin; cytokeratin; immunonanoparticles

Correspondence
J. Kos, Department of Pharmaceutical Biology, University of Ljubljana, Askerceva 7, 1000 Ljubljana, Slovenia
Fax: +386 1425 80 31
Tel: +386 40 792 639
E-mail: janko.kos@ffa.uni-lj.si
Website: http://www.ffa.uni-lj.si/index.php/content/view/full/107

(Received 25 April 2007, revised 19 June 2007, accepted 2 July 2007)

doi:10.1111/j.1742-4658.2007.05971.x

Breast cancer cells exhibit excessive proteolysis, which is responsible for extensive extracellular matrix degradation, invasion and metastasis. Besides other proteases, lysosomal cysteine protease cathepsin B has been implicated in these processes and the impairment of its intracellular activity was suggested to reduce harmful proteolysis and hence diminish progression of breast tumors. Here, we present an effective system composed of poly(D,L-lactide-coglycolide) nanoparticles, a specific anti-cytokeratin monoclonal IgG and cystatin, a potent protease inhibitor, that can neutralize the excessive intracellular proteolytic activity as well as invasive potential of breast tumor cells. The delivery system distinguishes between breast and other cells due to the monoclonal antibody specifically recognizing cytokeratines on the membrane of breast tumor cells. Bound nanoparticles are rapidly internalized by means of endocytosis releasing the inhibitor cargo within the lysosomes. This enables intracellular cathepsin B proteolytic activity to be inhibited, reducing the invasive and metastatic potential of tumor cells without affecting proteolytic functions in normal cells and processes. This approach may be applied for treatment of breast and other tumors in which intracellular proteolytic activity is a part of the process of malignant progression.

Cysteine cathepsins, an important group of lysosomal proteolytic enzymes [1,2], have been implicated in a number of steps in tumor progression, including processes of cell transformation and differentiation, motility, adhesion, invasion, angiogenesis and metastasis [3,4]. In particular, high activity of cathepsin B has been identified as an important tumor promoting factor capable of degrading proteins of the basement membrane and extracellular matrix (ECM) and enhancing progression of malignant disease. It has been demonstrated that, besides the extracellular cathepsin B, its intracellular fraction is involved in degrading the ECM, which is internalized by tumor cells and exposed to lysosomes [5,6].

We and others have demonstrated that inhibitors that are able to enter cells, and thus inactivate lysosomal cathepsin B, effectively reduce ECM degradation and consequently cell invasiveness [6]. However, the uptake by aggressive tumor cells of cathepsin B inhibitors, either small molecules, protein inhibitors or neutralizing monoclonal antibodies, is a rather slow process with very limited final efficacy. A strategy to speed up the uptake and to target the inhibitors to the lysosomes would be most desirable. Cathepsin B, however, possesses several functions with respect to physiological processes of normal cells, such as intracellular protein catabolism, pro-hormone processing and regulation of cytotoxic immunity [7–9], which should not

Abbreviations
ECM, extracellular matrix; EDC, 1-ethyl-3-(3-dimethylaminopopyl)carbodiimide hydrocloride; FITC, fluorescein isothiocyanate; PLGA, poly(D,L-lactide-coglycolide); TAA, tumor-associated antigen.

be affected during the treatment with the inhibitor. To direct the inhibitor therapy to the desired lysosomal-associated fraction of cathepsin B in tumor cells, a delivery system able to recognize and enter tumor cells, accumulating in the lysosomes, is necessary.

Polymeric nanoparticles comprise promising systems for delivering antitumor agents known for their rapid internalization into highly metabolizing cells by means of endocytosis. Moreover, they can protect the drug from premature degradation and control its release at the site of action, enhancing therapeutic efficacy and reducing undesirable side-effects [10]. Accumulation of nanoparticles in tumors is also a consequence of the enhanced permeation and retention effect resulting from the leakiness of tumor vasculature, poor blood flow, impaired lymphatic drainage and interstitial tumor pressure [11]. Another important application of polymeric nanoparticles as a carrier system is their ability to bind specific recognition molecules, which enables nanoparticles to be targeted specifically [12]. These ligands are usually mAbs that recognize tumor associated antigens (TAAs) that are expressed uniquely on the plasma membrane of targeted tumor cells. TAAs can be receptors, enzymes, glycoproteins, structural proteins, or other molecules localized predominantly on the tumor cell surface. In breast cancer, several candidates have been proposed as TAAs, such as EGFR/HER-2 [13], p53 and VEGF [14], which play important roles during the progression of the disease. However, these antigens are not completely specific to breast tumor cells and are also expressed in other human tissues.

In the present study, we loaded poly(D,L-lactide-coglycolide) (PLGA) nanoparticles with potent cysteine protease inhibitor cystatin and labeled the delivery system with the mAb recognizing specific profile of cytokeratins overexpressed in breast tumor cells. Selective cellular uptake of the delivery system was tested in cocultures of invasive breast cells (MCF-10A neoT) with enterocytes (Caco-2) and monocytes/macrophages (U-937). Additionally, we evaluated the effect of loaded cystatin to impair lysosomal proteolytic activity and invasive potential in targeted cells.

Results

Antibody characteristics and preparation of antibody-coated nanoparticles

Antigen specificity was determined on the cell lysates of MCF-7 and MCF-10A neoT cells using indirect ELISA. Anti-cytokeratin monoclonal IgG showed concentration dependent binding to both cell lysates. Greater affinity was observed against MCF-7 cells than to MCF-10A neoT cells (data not shown). The antibody recognizes a specific cytokeratin profile (cytokeratines 1, 2, 8, 10, 18) as determined by 2D electrophoresis, immunoblot and mass spectroscopy (unpublished results).

Immunocytochemical analysis of MCF-10A neoT cells showed the localization of mAb antigen on the plasma membrane. The incubation of nonpermeabilized MCF-10A neoT cells with anti-cytokeratin monoclonal IgG allowed a staining of the antigen as a rim at the plasma membrane (Fig. 1A–C). However, when cells were permeabilized with Triton X-100, a cytoplasmic antigen was stained organized into a thin, 3D network within the entire cells (data not shown).

Nanoparticles produced exhibited a mean diameter of 320–360 nm with a polydispersity index of 0.34. The mean zeta potential of nanoparticles was −25 mV. Nanoparticles were coated with anti-cytokeratin monoclonal IgG using the adsorbtion method, preserving biological activity of bound mAb [15]. Coating efficiency was proven either by the use of Alexa 546 labeled anti-cytokeratin monoclonal IgG or Alexa 546 labeled secondary antibody (Fig. 1D). As observed from Fig. 1D, fluorescein isothiocyanate (FITC)-loaded nanoparticles were efficiently labeled with anti-cytokeratin monoclonal IgG. The result was confirmed by measurement of the intensities of Alexa 546 fluorescence relative to FITC fluorescence using the fluorescence microtiter plate reader. The intensity of Alexa 546 fluorescence was shown to be dependent on the ratio between nanoparticles and the labeling antibody [15].

Surface plasmon resonance

To confirm the binding of anti-cytokeratin monoclonal IgG to the nanoparticles, the nanoparticles were tested for their interaction with protein A, immobilized onto the surface of an SA sensor chip. In case of anti-cytokeratin monoclonal IgG-coated nanoparticles, a strong interaction was observed, due to interaction between the Fc region of anti-cytokeratin monoclonal IgG adsorbed onto the nanoparticles and protein A bound on the chip. (Fig. 2A). The noncoated nanoparticles, however, did not provide any significant signal (Fig. 2B). As a control, the antibody solution was tested for interaction with protein A and, as expected, showed an interaction with protein A (Fig. 2C).

Internalization of nanoparticles

The uptake of nanoparticles, loaded with FITC and coated with anti-cytokeratin monoclonal IgG, into MCF-10A neoT cells, in comparison to noncoated

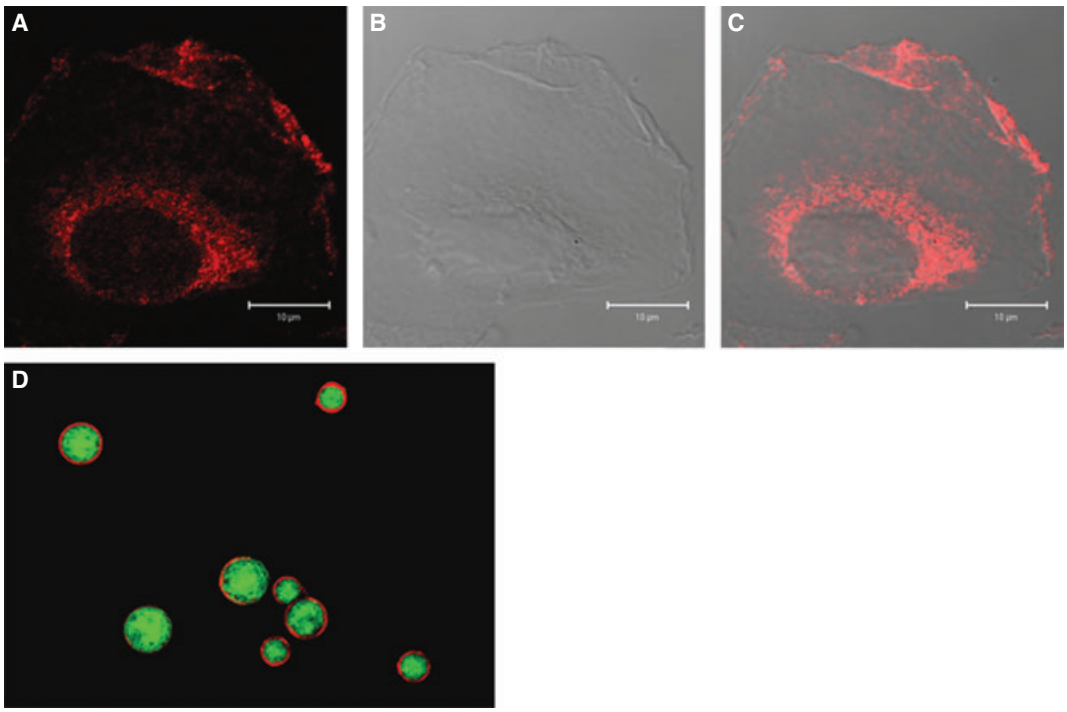

Fig. 1. Localization of anti-cytokeratin monoclonal IgG antigens and antibody-coated nanoparticles. (A–C) Localization of cytokeratines on cell membrane of MCF-10A neoT cells with anti-cytokeratin monoclonal IgG. MCF-10A neoT cells were grown on coverslips for 24 h and fixed with paraformaldehide. Before labeling, nonspecific staining was blocked with 3% BSA. (A) MCF-10A neoT cells stained with Alexa 546 labeled anti-cytokeratin monoclonal IgG. (B) Differential interference contrast of MCF-10A neoT cells. (C) Superimposed image of (A) and (B). (D) PLGA micro- and nanoparticles with incorporated FITC (green fluorescence) and coated with anti-cytokeratin monoclonal IgG (red fluorescence). Due to visualization, larger particles in diameter up to 1–2 μm were selected. To determine the coating efficiency, the antibody was detected with Alexa 546-labeled secondary anti-mouse IgG.

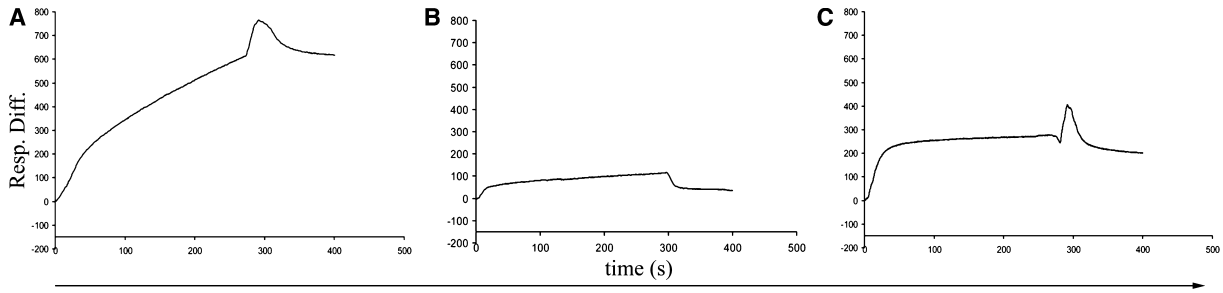

Fig. 2. Surface plasmon resonance analysis of the interaction of anti-cytokeratin monoclonal IgG-coated nanoparticles with immobilized protein A on an SA sensor chip. (A) Anti-cytokeratin monoclonal IgG-coated nanoparticles, strongly interacting with protein A. (B) Noncoated nanoparticles without significant binding. (C) Anti-cytokeratin monoclonal IgG.

nanoparticles, was monitored by fluorescence microscopy. The uptake for nanoparticles coated with the anti-cytokeratin monoclonal IgG was comparable to that the noncoated nanoparticles (Fig. 3). After the internalization of coated nanoparticles, green FITC fluorescence could be observed in the perinuclear region, corresponding to lysosomal vesicles, similarly to internalized noncoated nanoparticles.

Internalization process was also observed in a coculture of MCF-10A neoT and Caco-2 cells. Nanoparticles coated with anti-cytokeratin monoclonal IgG entered solely MCF-10A NeoT cells and not Caco-2 cells, showing specific localization in the targeted cells (Fig. 4). Noncoated nanoparticles, however, did enter both Caco-2 and MCF-10A neoT cells, revealing their nonselective uptake (Fig. 4).

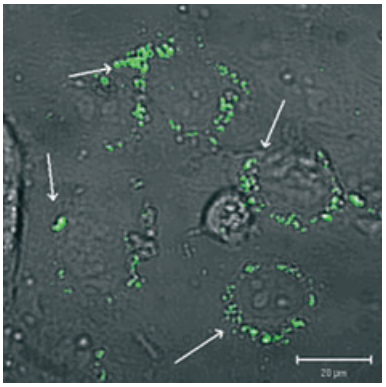

Fig. 3. Internalization of antibody-coated nanoparticles into MCF-10A neoT cells. The cells were exposed to the nanoparticles for up to 8 h. Arrows show the intracellular localization of nanoparticles in the vesicles in the perinuclear area. Green fluorescence corresponds to the incorporated FITC.

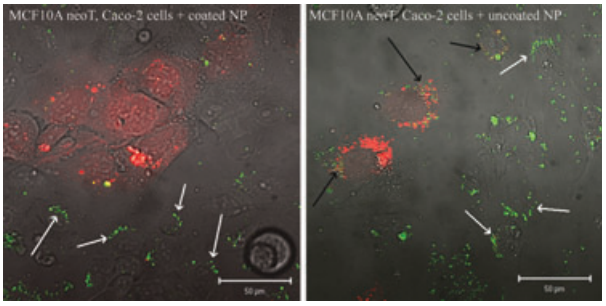

Fig. 4. Internalization of antibody-coated nanoparticles (left) and uncoated nanoparticles (right) into MCF-10A neoT cells and Caco-2 cells, the latter labeled with Orange Cell Tracker. Green fluorescence corresponds to FITC, incorporated into nanoparticles. Uncoated nanoparticles did enter Caco-2 cells (black arrows) as well as MCF-10A neoT cells (white arrows), exhibiting nonspecific uptake by both cell lines (right). Antibody-coated nanoparticles entered solely MCF-10A neoT cells (white arrows) (left).

Flow cytometry

Internalization of nanoparticles into MCF-10A neoT cells at different time points was followed by flow cytometry. Under our experimental conditions, noncoated nanoparticles and anti-cytokeratin-coated nanoparticles entered 58.58% and 64.72% of cells within 1 h, respectively, whereas the percentage increased to 77.40% and 80.93% within 8 h of incubation, respectively. After 24 h, more than 90% of cells internalized noncoated as well as anti-cytokeratin monoclonal IgG-coated nanoparticles (Fig. 5).

In a coculture of MCF-10A neoT and Caco-2 cells, MCF-10A neoT cells internalized nanoparticles (Fig. 6A), observed as a shift in green fluorescence

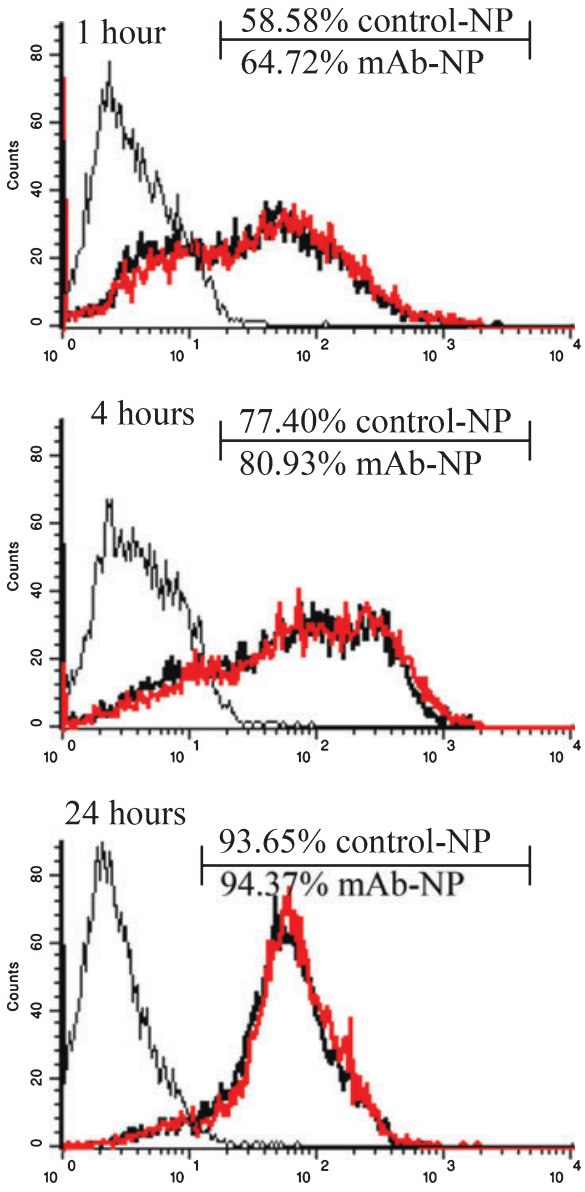

Fig. 5. Flow cytometry of MCF-10A neoT cells. The cells were incubated with anti-cytokeratin monoclonal IgG-coated or noncoated nanoparticles loaded with cystatin for 1, 4 and 24 h, prior the analysis. Internalization of mAb-coated nanoparticles into MCF-10A neoT can be seen as a shift in fluorescence intensity (thick red line) in comparison to internalization of noncoated nanoparticles (thick black line). As a control, MCF-10A neoT cells were grown in the absence of nanoparticles (thin black line). The percentages indicate the proportion of MCF-10A neoT cells that have internalized noncoated and mAb-coated nanoparticles, respectively.

intensity due to internalization of FITC-loaded nanoparticles. Caco-2 cells, however, in a coculture with MCF-10A neoT cells, did not internalize anti-cytokeratin monoclonal IgG labeled nanoparticles (Fig. 6B).

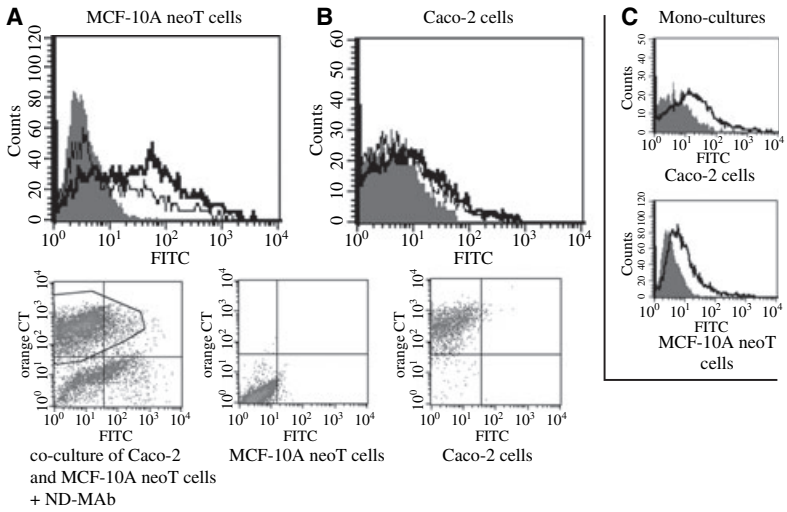

Fig. 6. Flow cytometry of a coculture of MCF-10A neoT cells and Caco-2 cells. The cells were incubated with anti-cytokeratin monoclonal IgG-coated nanoparticles loaded with cystatin for 1 h prior the analysis. Internalization of nanoparticles into MCF-10A neoT can be seen as a shift in fluorescence intensity (thick line) in comparison to MCF-10A neoT cells grown in the absence of nanoparticles (thin line) (A). Caco-2 cells, however, did not internalize antibody-coated nanoparticles and, consequently, there is no shift in a fluorescence intensity between Caco-2 cells grown in the presence (thick line) or the absence (thin line) of nanoparticles (B). In a monoculture, however, both MCF-10A neoT cells and Caco-2 cells internalized anti-cytokeratin monoclonal IgG-coated nanoparticles (C).

This result confirms the specific uptake of anti-cytokeratin monoclonal IgG-coated nanoparticles by MCF-10A neoT cells, whereas Caco-2 cells did not show any shift in fluorescence, indicating an absence of nanoparticle uptake. In a monoculture, however, both Caco-2 and MCF-10A neoT cells internalized anti-cytokeratin monoclonal IgG-coated nanoparticles to a similar extent (Fig. 6C).

Proteolysis assay

The capability of cystatin-loaded, antibody-coated nanoparticles to inhibit intracellular proteolytic activity in living MCF-10A neoT cells was tested by using specific cathepsin B fluorogenic substrate Z-Arg-Arg cresyl violet. Since cathepsin B is highly concentrated in lysosomes in MCF-10A neoT cells, a strong red fluorescence of the degraded substrate appeared in the vesicles in the perinuclear region immediately after treatment with the substrate (Fig. 7). The fluorescence matched the intracellular localization of cathepsin B well, confirming that a large part of the lysosomal cathepsin B was present in its active form [16].

Preincubation of cells with cystatin-loaded, anti-cytokeratin monoclonal IgG-coated nanoparticles almost completely abolished the substrate fluorescence, showing that cathepsin B activity was strongly inhibited. The amount of cystatin released from the nanoparticels during the preincubation period was

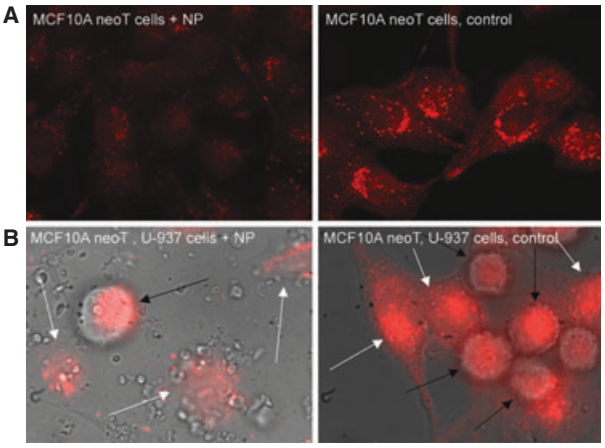

Fig. 7. Inhibition of cathepsin B activity with antibody-coated nanoparticles loaded with cystatin as determined by Z-Arg-Arg cresyl violet degradation. MCF-10A neoT cells were incubated with the nanoparticles for 2 h in serum free medium (left row), either in a monoculture (A) or in a coculture with differentiated U-937 cells (B). Prior to the assay, cells were washed and Z-Arg-Arg substrate was added (10 μM). Red fluorescence of the degradation product was observed after 15 min. The controls were preincubated with serum free medium in the absence of nanoparticles (right row). The cathepsin B activity was significantly reduced in MCF-10A neoT cells preincubated with the cystatin-loaded nanoparticles compared to controls (A). In a coculture, the activity of cathepsin B was reduced only in MCF-10A neoT cells (white arrows) and not in U-937 cells (black arrows) (B), suggesting that the nanoparticles were internalized to MCF-10A neoT cells due to the specific targeting of anti-cytokeratin monoclonal IgG.

negligible, as determined from the loading capacity and a release profile. As shown in our previous study [16], the free cystatin added to the MCF-10A neoT cells was not effective against intracellular cathepsin B. Furthermore, nanoparticles and cystatin did not exhibit any cytotoxic effect within concentration range used in experiments. The instrument settings, such as intensity of excitation light, magnification and exposure time on digital camera, were kept constant following the inhibition of cathepsin B activity.

In a coculture system of MCF-10A neoT and differentiated U-937 cells, cathepsin B activity was significantly reduced only in MCF-10A neoT cells and not in differentiated macrophages when cystatin-loaded anti-cytokeratin nanoparticles were applied (Fig. 7). Like MCF-10A neoT cells, differentiated U-937 cells also express high levels of active cathepsin B. The red fluorescence in MCF-10A neoT cells was restored after a prolonged time of incubation with cathepsin B specific substrate, showing that the integrity of cells was preserved. As shown in our previous study [16], the nanoparticles do not effect the cells viability after internalization, but merely deliver the inhibitor to the lysosomal targets.

Invasion assay

The effect of cystatin incorporated into nanoparticles on the Matrigel invasion of MCF-10A neoT cells was tested after a 24 h incubation period. Free cystatin decreased the invasion of MCF-10A neoT cells to 87.65% compared to the control with the absence of inhibitor ($P = 0.02$). Cystatin incorporated in nanoparticles was, however, more efficient and reduced the invasiveness to 71.8% of the control ($P = 0.002$) (Fig. 8). The efficacy of the invasion in the control experiment was 29.65%. This result shows that effective inhibition of intracellular proteolytic activity additionally reduces invasive potential of MCF-10A neoT cells and emphasizes one of the adventages of the new delivery system (i.e. its rapid internalization).

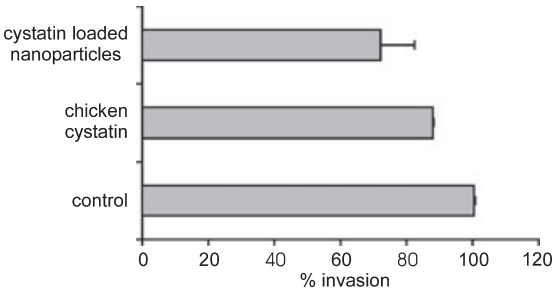

Fig. 8. Effect of chicken cystatin on Matrigel invasion by MCF-10A neoT cells. Cells were incubated for 24 h in the presence of chicken cystatin, either incorporated in nanoparticles (50 μg nanoparticles·mL^{-1}) or free (2 μM) in the serum medium depleted of protease inhibitors. The efficacy of the invasion in the absence of inhibitors was 29.6%. Data are represented as the means ± SD of two independent determinations performed in triplicate.

Discussion

In our previous study [16], a nanoparticulate carrier system was used to deliver the potential antitumor drug cystatin to transformed breast epithelial MCF-10A neoT cells. Using such a delivery system, we showed that the uptake of the drug by targeted cells was significantly increased. Moreover, PLGA biodegradable polymers also protected cystatin against proteolytic degradation and aggregation and enabled its sustained release inside the cells. Although PLGA nanoparticles can be concentrated in tumor tissue due to the enhanced permeation and retention effect and enhanced internalization by endocytosis, their uptake cannot be excluded for other cells and, thus, the delivery of antitumor drug is not specific.

To improve the specificity of the carrier system towards the breast tumor cells, nanoparticles were coated with a specific monoclonal antibody [17,18] directed against TAAs (Fig. 9). As noted above, there are several candidates for TAAs in breast cancer, however, none of them is specific only for breast tumor cells, and is expressed as well in other tumors or normal human tissues. Thus, the antibodies, developed against these antigens and used in cell targeting are only as specific as the expression of the antigen itself. The other approach to raising antibodies, specific to tumor cells is to apply tumor cell extract for immunization of animals [19,20]. The mAb used for specific targeting in the present study was raised against soluble membrane proteins of MCF-7 cells obtained from human invasive ductal breast carcinoma. Immunohistochemical analysis showed specific staining for breast tumors: positive staining was detected mostly in primary breast carcinomas and in lymph node metastasis [21]. No immunostaining was detected in other tumor types, other than melanoma. Tumor cell lines show a similar pattern of reactivity: positive immunostaining was detected only with breast carcinoma cells and melanoma cells [21]. As shown in our recent study, the antibody recognizes a specific membrane cytokeratin profile (cytokeratins 1, 2, 8, 10 and 18) expressed by MCF-7 and other invasive breast cells, including our test cell line MCF-10A neoT (B. Dolsak, N. Oberhaser & J. Kos, unpublished results). Besides the mouse monoclonal antibody used in the present study its

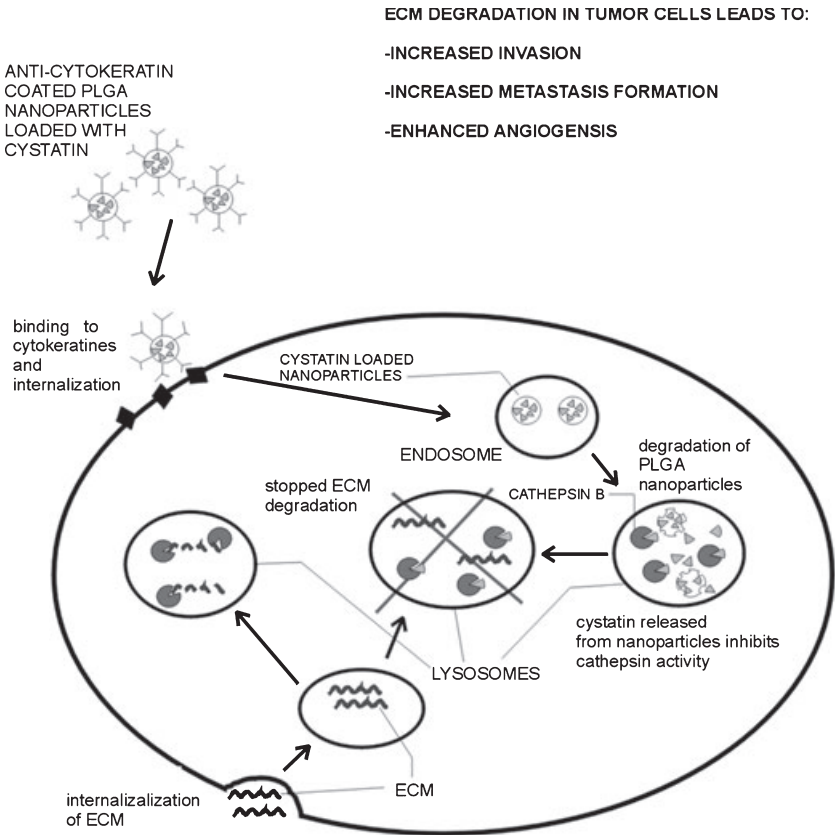

Fig. 9. Mechanism of nanoparticle cellular uptake and impairment of lysosomal proteolytic activity of cysteine protease cathepsin B in targeted cells. An important feature of the invasive breast cancer cell phenotype is an excessive intracellular proteolytic activity of cysteine proteases, resulting in the degradation of extracellular matrix. Cysteine protease inhibitors are capable of imparing the degradation of the ECM, and thereby reducing the invasive potential of tumor cells. Chicken cystatin has a high potential for inactivating cathepsin B, however, free cystatin is unable to enter the cells and inhibit intracellular proteolytic activity. Incorporation of cystatin into the biodegradable nanoparticles enables its internalization, release and inhibition of cathepsin B activity in the lysosomes. Furthermore, the labeling of nanoparticles with anti-cytokeratin monoclonal IgG provides specific delivery of nanoparticles to the epithelial breast cancer cells.

humanized analogue has been prepared, enabling potential *in vivo* application [22].

Cytokeratins are being used extensively for tumor diagnosis in various types of malignancy [23]. Cytokeratins expressed by primary tumor cells [24] also remain present in invasive and metastatic cells, which additionally makes them good markers for local invasions and distant metastases [25]. Moreover, aggressive tumors with the poorest clinical outcome, such as basal-like breast carcinomas [26], express a typical cytokeratin profile, distinct from that in less aggressive ones. Therefore, the differential expression of individual cytokeratins in various types of carcinomas makes these proteins useful targets [27] for specific drug delivery in cancer patients.

We bound anti-cytokeratin monoclonal IgG to the surface of PLGA nanoparticles either by adsorption and covalently, using 1-ethyl-3-(3-dimethylaminopopyl)carbodiimide hydrocloride (EDC) as the bifunctional reagent. The antibody adsorbed effectively to the surface of the nanoparticles, as shown by fluorescence labeling, surface plasmon resonance and flow cytometry. The biological activity of the adsorbed antibody was fully preserved, as shown by its binding capacity to MCF-7 and MCF-10A neoT cell lysates. By contrast, when bound covalently to the nanoparticles using EDC as a bifunctional reagent, the antibody was completely inactive [15].

Successful internalization and lysosome targeting should be an important advantage of our new delivery system. Our strategy relies on the ability of targeting agent to bind to the tumor cell surface and to trigger receptor-dependent endocytosis resulting in the delivery of the therapeutic agent to the endosomes and lysosomes. Polymeric nanoparticles themselves are internalized by clathrin-mediated endocytosis [28], which is significantly enhanced in highly proliferating tumor cells [29]. Our nanoparticulate delivery system, coated with the antibody showed a similar internalization profile compared to noncoated nanoparticles, as shown by confocal microscopy and flow cytometry. Since the final destination of the antibody-coated nanoparticles was endosomes and lysosomes, as seen from vesicular fluorescence in the perinuclear region, we may speculate that the antibody-coated nanoparticles explored the same receptor-dependent endocytosis pathway. The presence of predominantly uncoated nanoparticles inside the cells, as shown by fluorescence microscopy (data not shown) support this pathway. Thus, our results reveal that anti-cytokeratin-coated

nanoparticulate delivery system is able to reach lysosomal protein targets in MCF-10A neoT cells.

The selectivity of the new delivery system was tested in a coculture of invasive breast cells (MCF-10A neoT) and enterocytes (Caco-2) using fluorescence microscopy and flow cytometry. By fluorescence microscopy, we observed that the noncoated nanoparticles entered both types of cells, indicating nonselective uptake. However, nanoparticles coated with the antibody only entered the MCF-10A neoT cells and not the Caco-2 cells demonstrating selectivity in their cell localization. In a monoculture, however, anti-cytokeratin monoclonal IgG-coated nanoparticles entered both Caco-2 and MCF-10A neoT cells. This is in line with previous studies showing that Caco-2 cells efficiently internalize nanoparticles [30] and demonstrates that selective uptake of nanoparticles can only be achieved when they are targeted to antigen expressing cells.

The final goal of our study was to prove that the inhibitor cargo (i.e. cystatin) delivered by our system to endosomes and lysosomes in breast tumor cells is capable of inactivating the raised intracellular proteolytic activity specifically in breast tumor cells, thereby reducing the invasive potential of the cells. The uptake of chicken cystatin, an analogue of human cystatin C and a potent inhibitor of cathepsin B, was tested by the inhibition of cathepsin B proteolytic activity, using the specific cathepsin B fluorogenic substrate Z-Arg-Arg cresyl violet. Since cathepsin B is highly concentrated in the lysosomes in MCF-10A neoT cells, it exhibits a strong red fluorescence in the vesicles in the perinuclear region after treatment with the substrate. When the cells were pretreated with the immunonanoparticles, loaded with the cystatin, red fluorescence diminished demonstrating effective uptake of cystatin and inhibition of the intracellular cathepsin B.

The effectiveness of the new delivery system to inhibit intracellular proteolytic activity selectively in breast MCF-10A neoT cells was evident when they were cocultured with Caco-2 cells that themselves express low levels of cysteine proteases. The selectivity of this system was further emphasized when MCF-10A neoT cells were cocultured with differentiated monocyte/macrophage U-937 cells, which can internalize PLGA nanoparticles [31] and which contain large amounts of cysteine proteases, including cathepsin B. Although differentiated U-937 cells can internalize PLGA nanoparticles more efficiently than Caco-2 cells [30], the activity of cathepsin B in differentiated U-937 cells was not lowered when the cells were preincubated with antibody-coated, cystatin-loaded nanoparticles. On the other hand, the activity was markedly reduced in MCF-10A neoT cells.

The preference of rapid internalization of cysteine protease inhibitor into MCF-10A neoT cells by the new delivery system and its ability to inhibit proteolytic activity was further demonstrated in a Matrigel invasion assay. Cystatin incorporated in nanoparticles reduced the invasion of MCF-10A neoT cells significantly better than the free cystatin. As the free cystatin is internalized very slowly and is unable to impair intracellular proteolytic activity [16], the difference in cell invasiveness can be attributed to efficient impairment of intracellular cysteine proteases by cystatin released in lysosomes from the nanoparticulate delivery system.

In summary, a new delivery system is described, comprising biodegradable PLGA polymeric nanoparticles, potent protease inhibitor cystatin and a specific anti-cytokeratin monoclonal IgG, which can be internalized into cells, contributes specific targeting to invasive breast epithelial cells and inactivates intracellular cathepsin B. This enables the tumor associated proteolytic activity to be inhibited, reducing the invasive and metastatic potential of tumor cells without affecting proteolytic functions in normal cells and processes. This new method of tumor targeting can be applied using other protease inhibitors and antibodies against other tumor associated antigens. The method has the potential to improve the efficacy and decrease the toxicity of existing and novel anticancer therapies.

Experimental procedures

Cell culture

MCF-10A neoT cells were provided by BF Sloane (Wayne State University, Detroit, MI, USA). Their origin was a human breast epithelial cell line (MCF-10) transformed with a neomycin resistance gene and c-Ha-ras oncogene. MCF-7 cells were obtained from ATCC (HTB 22) (Rockville, MD, USA). Cells were cultured in a monolayer to 80% confluence in Dulbecco's modified Eagle's medium (DMEM)/F12 medium supplemented with 12.5 mM Hepes, 2 mM glutamine, Sigma (St Louis, MO, USA), 5% fetal bovine serum, HyClone (Logan, UT, USA), insulin, hydrocortisone, epidermal growth factor and antibiotics, at 37 °C in a humidified atmosphere containing 5% CO_2. Prior to use in an assay, cells were detached from culture flasks with 0.05% trypsin and 0.02% EDTA in NaCl/P_i, pH 7.4. The viability of cells in the experiments was at least 90%, as determined by staining with nigrosin. Caco-2 cells were cultured in minimal essential medium supplemented with 2 mM glutamine, 1% nonessential amino acids and 10%

fetal bovine serum. U-937 cells were obtained from ATCC (CRL 1593) and cultured in advanced RPMI-1640 medium with 2 mM glutamine, 5% fetal bovine serum and antibiotics.

Antibody preparation

The mouse monoclonal antibody, used in this study, was raised against soluble membrane proteins of MCF-7 human invasive ductal breast carcinoma. Using immunocytochemical analysis, its positive staining was detected predominantly in primary breast carcinomas and in metastatic lymph nodes [21]. Hybridoma cells for antibody isolation were cultured in DMEM medium supplemented with 2 mM glutamine (Sigma), 13% fetal bovine serum (HyClone) and antibiotics, at 37 °C in a humidified atmosphere containing 5% CO_2. The antibody was isolated by affinity chromatography on protein A sepharose using standard procedure and labeled with Alexa 546 fluorescent dye according to the manufacturer's instructions (Molecular Probes, Carlsbad, CA, USA). The labeled antibody was stored at −20 °C.

Immunofluorescence

For immunofluorescence detection, MCF-10A neoT cells were cultured on glass coverslips to 70% confluence. To preserve membrane associated components and foreclose cytoplasmic staining, cells were fixed with 2% paraformaldehide at room temperature for 10 min. Nonspecific staining was blocked with 3% BSA in phosphate buffer saline ($NaCl/P_i$), pH 7.4, for 1 h. After 1.5 h of incubation with Alexa 546-labeled anti-cytokeratin monoclonal IgG, cells were washed with $NaCl/P_i$. The Prolong Antifade kit (Molecular Probes) was used for mounting coverslips on glass slides. Fluorescence microscopy was performed using Carl Zeiss LSM 510 confocal microscope (Carl Zeiss, Oberkochen, Germany). Alexa 546 was excited with an He/Ne (543 nm) laser and emission was filtered using narrow band LP 560 nm filter. Images were analyzed using Carl Zeiss LSM image software, version 3.0.

Preparation of antibody-coated nanoparticles loaded with cystatin

Nanoparticles were prepared by the double emulsion solvent diffusion method under mild experimental conditions as described [16]. Chicken cystatin [32], either labeled with Alexa 488 dye or unlabeled was dissolved in deionized water and dispersed in ethyl acetate containing PLGA (lactic acid/glycolic acid (50 : 50, w/w) copolymers; Resomer RG®, Boehringer, Germany). Alternatively, 1.7 mg of FITC solution (4.26 $mg \cdot mL^{-1}$) was added to ethyl acetate containing PLGA copolymers.

The copolymers contained free (RG® 503 H with MW 48 kDa) carboxyl end groups. After emulsification in combination with sonication 5% PVA in aqueous solution (Mowiol® 4-98; Hoechst, Germany) was added to the water-in-oil emulsion to form a double emulsion (w/o/w). The organic solvent was removed by extraction with 0.1% PVA in aqueous solution in homogenizer with stirring at 3214 ***g*** for 5 min. The resulting nanoparticles were washed and recovered by centrifugation at 25 283 ***g*** for 15 min (ultracentrifuge Sorvall RC 5C Plus, Norwalk, CT, USA). The sediment was re-dispersed by bath sonication. Finally, the aqueous dispersion of purified nanoparticles was filtered through a membrane, pore size 12–35 μm (Shleicher & Schuell, Dassel, Germany) to remove aggregates formed during the purification process. If not used for antibody coating the same day, the samples were placed in liquid nitrogen and freeze-dried (Heto FD3, Heto-Holten A/S, Allerød, Denmark).

Nanoparticles were coated with anti-cytokeratin monoclonal IgG using the adsorbtion method [15]. Dispersed nanoparticles were incubated overnight with the antibody (0.85 : 1, w/w), pH 5.0, and 4 °C. In a control experiment, the nanoparticles were incubated in the absence of antibody in the same volume of the buffer. The nanoparticles were then washed twice with $NaCl/P_i$, pH 5.0 and recovered by centrifugation at 12 857 ***g*** for 15 min (Ultracentrifuge Sorvall RC 5C Plus). For covalent binding of anti-cytokeratin monoclonal IgG, EDC reagent was used [15].

Either Alexa 546 labeled anti-cytokeratin monoclonal IgG or, alternatively, secondary goat anti-mouse serum labeled with Alexa 546 was used to determine the coating efficiency. When Alexa 546 labeled secondary antibody was used to detect the mAb adsorbed to PLGA nanoparticles, the system was incubated with the secondary antibody (1 : 1000) for 2 h at room temperature, washed twice with $NaCl/P_i$, pH 5.0 and recovered by centrifugation at 12 857 ***g*** for 15 min (Ultracentrifuge Sorvall RC 5C Plus). In a control experiment, nonderivatized nanoparticles were incubated with the secondary antibody. Fluorescence microscopy was performed using Carl Zeiss LSM 510 confocal microscope under the conditions described above.

Surface plasmon resonance

The coating efficiency of nanoparticles with anti-cytokeratin monoclonal IgG was monitored using Biacore X system (BIAcore, Uppsala, Sweden). Assays were performed on a SA sensor chip that contains preimmobilized streptavidin on its surface (BR-1003-98 BIAcore). Biotinilated protein A was immobilized onto streptavidin at a flow rate 1 $\mu L \cdot min^{-1}$ for 10 min (300 RU). The reference cell was blocked with biotin (10 μM, 10 min). The chip was then washed with 5 μL of 10 mM glycine buffer (pH 2.2) at a flow rate of 30 $\mu L \cdot min^{-1}$. Identical wash cycles were used to regenerate

the chip between assays. Nanoparticles labeled with anti-cytokeratin monoclonal IgG or nonlabeled nanoparticles were prepared in PBST buffer (NaCl/P_i with 0.05% Tween 20). All steps were performed at 25 °C with a flow rate of 1 μL·min^{-1} in 1% PBST running buffer; 5 μL of nanoparticle suspension was injected for each assay. As a control, anti-cytokeratin monoclonal IgG was injected with a flow rate of 1 μL·min^{-1} in 1% PBST running buffer.

Internalization assay

MCF-10A neoT cells were placed in LabTek chambered coverglass system (Nalge Nunc International, Rochester, NY, USA) at a concentration of 1×10^5·mL^{-1} and allowed to attach. In a coculture experiment, Caco-2 cells were grown to 80% confluence in six well plates (Corning Costar, Cambridge, MA, USA). Prior to labeling, the medium was removed and the cells washed with NaCl/P_i. The medium with 10 μM Orange Cell Tracker (Molecular Probes) was added and cells were incubated for 40 min. The medium was changed and the cells incubated for another 30 min. The cells were then detached and placed in the LabTek chambered coverglass system (Nalge Nunc International) at a concentration of 1×10^5/mL in a coculture with MCF-10 A neoT cells and allowed to attach. Nanoparticles labeled with FITC were added and the cells were observed for particle internalization. Nanoparticles incubated in the absence of anti-cytokeratin monoclonal IgG were used as a control. As the nanoparticles in the presence or absence of antibodies were prepared, incubated and washed identically, we can exclude the possibility that the difference in cell uptake depends on FITC loading of nanoparticles. The internalization of nanoparticles was confirmed also by fluorescence spectrometry [15].

Fluorescence microscopy was performed using a Carl Zeiss LSM 510 confocal microscope. FITC and Orange Cell Tracker were excited with an argon or He/Ne laser and emission was filtered using a narrow band LP 505–530 nm (green fluorescence) and 560 nm (red fluorescence) filter, respectively.

Flow cytometry

Internalization of anti-cytokeratin monoclonal IgG-coated nanoparticles was observed by flow cytometry by a shift in a fluorescence intensity. MCF-10A neoT cells were placed into six well plates and allowed to attach. Afterwards, FITC-loaded nanoparticles labeled with anti-cytokeratin monoclonal IgG were added and the cells were incubated for different time periods.

To determine specific uptake, MCF-10A neoT and Caco-2 cells were plated either in a mono- or coculture. In both cases, the total cell number in each well was 4×10^5. Prior to the assay, Caco-2 cells were labeled with Orange Cell Tracker as described above to facilitate differentiation between the two cell lines. Next, Alexa 488 labeled-cystatin-loaded nanoparticles (see proteolysis assay) labeled with anti-cytokeratin monoclonal IgG were added and the cells were incubated for 4 h. As a control, cells were grown separately in a monoculture in the absence of nanoparticles. Flow cytometry was performed on a FACS Calibur (Beckton Dickinson, Inc., Franklin Lakes, NJ, USA).

Proteolysis assay

A specific fluorogenic substrate, Z-Arg-Arg cresyl violet, was used to detect intracellular proteolytic activity of cathepsin B and the inhibitory effect of cystatin [16]. Cleveage by cathepsin B of one or both arginine residues converts the molecule into a red fluorescent product [5]. The substrate easily penetrates the cell membrane, and intracellular cathepsin B activity is identified after a short incubation period.

Cells were grown in a chambered coverglass system (Lab-Tek, Nalge Nunc International) as described above. Before the assay, culture medium was removed and the cells washed twice with NaCl/P_i. The cells were then preincubated for 2 h with antibody-coated nanoparticles loaded with cystatin in serum free culture medium. Control cells were incubated in the absence of the nanoparticles. After incubation, the inhibitor solution was removed from the cells and substituted by the substrate (10 mM in serum free medium) and monitored for fluorescent product.

To determine specific delivery of anti-cytokeratin monoclonal IgG-labeled nanoparticles and cell-specific inactivation of cathepsin B activity, MCF-10A neoT cells were grown in a coculture with differentiated U-937 monocytes/macrophages, that also exhibit a high level of cathepsin B activity. 4×10^5 U-937 cells·mL^{-1} were differentiated with 50 nM 4β-phorbol 12-myristate 13-acetate for 24 h. Cells were then washed with NaCl/P_i, pH 7.4, detached with 0.02% EDTA in NaCl/P_i, washed again with NaCl/P_i and added to the culture of MCF-10A neoT cells in the chambered coverglass system and allowed to adhere. Next, proteolysis was assayed as described for the monoculture of MCF-10A neoT cells. Fluorescence was measured using Carl Zeiss LSM 510 confocal microscope under the conditions described above, combined with a differential interference contrast imaging module.

Cell invasion assay

The effect of cystatin-loaded nanoparticles on invasion was tested using the modified method as previously described [33]. Transwells (Corning Costar) with 12-mm polycarbonate filters (12 μm pore size were used. Twenty-five μL of 100 μg·mL^{-1} fibronectin (Sigma) was applied on lower side of the filters and left for 1 h in a laminar hood to dry. Afterwards, the upper side of the filters was coated with 100 μL of 1 mg·mL^{-1} Matrigel (Beckton Dickinson, Inc.)

and 100 μL of DMEM was added. The Matrigel was dried overnight at room temperature in a laminar hood and reconstituted with 200 μL of DMEM at 37 °C for 1 h. The upper compartments were filled with 500 μL of MCF-10A neoT cells (4×10^5 cells·mL^{-1}), pretreated for 1 h with 2 μM chicken cystatin or 50 μg·mL^{-1} cystatin-loaded nanoparticles. The lower compartments were filled with 1.5 mL of medium. Either 2 μM concentration of chicken cystatin was added to upper and lower compartments or 50 μg·mL^{-1} cystatin-loaded nanoparticles were added to the upper compartment. The control cells were not pretreated and were plated in the absence of inhibitor. The plate were incubated for 24 h at 37 °C and 5% CO_2. 3-(4,5-Dimethylthiazol-2-yl)-2,5-diphenyl-tetrazolium bromide was added to a final concentration of 0.5 mg·mL^{-1} to the upper and lower compartments and the plate incubated for an additional 3 h. Media from both compartments were transferred separately to Eppendorf tubes and centrifuged at 6446 ***g*** for 5 min. Supernatants were discarded and the formazan crystals dissolved in isopropanol. The color intensity of the dissolved formazan was measured at 570 nm (reference filter 690 nm). Invasion was recorded as the percentage of the cells that penetrated the Matrigel-coated filters compared to controls. The SPSS software package (release 13.0; SPSS Inc., Chicago, IL, USA) was used for statistical analysis. The difference between the groups was evaluated using the nonparametric Mann–Whitney test. $P < 0.05$ was considered statistically significant.

Acknowledgements

The authors thank to Professor Roger Pain for critical reading of the manuscript and Professor Cornelius Van Noorden for providing the fluorogenic substrate Z-Arg-Arg cresyl violet. Surface plasmon resonance experiments were performed in the Infrastructural Centre for Surface Plasmon Resonance at the Department of Biology, University of Ljubljana. This work was supported by the Research Agency of the Republic of Slovenia and partially by the Sixth EU Framework IP project CancerDegradome.

References

1 Turk B (2006) Targeting proteases: successes, failures and future prospects. *Nat Rev Drug Discov* **5**, 785–799.
2 Mohamed MM & Sloane BF (2006) Cysteine cathepsins: multifunctional enzymes in cancer. *Nat Rev Cancer* **6**, 764–775.
3 Kos J & Lah TT (1998) Cysteine proteinases and their endogenous inhibitors: target proteins for prognosis, diagnosis and therapy in cancer. *Oncol Rep* **5**, 1349–1361.
4 Bervar A, Zajc I, Sever N, Katunama N, Sloane BF & Lah TT (2003) Invasiveness of transformed human breast epithelial cell lines is related to cathepsin B and inhibited by cysteine proteinase inhibitors. *Biol Chem* **383**, 447–455.
5 van Noorden CJF, Jonges GN, van Marle J, Bissell ER, Griffini P, Jans M, Snel J & Smith ER (1998) Heterogenous supression of experimentally induced colon cancer metastasis in rat liver lobes by inhibition of extracellular cathepsin B. *Clin Exp Metast* **16**, 159–167.
6 Premzl A, Zavasnik-Bergant T, Turk V & Kos J (2003) Intracellular and extracellular cathepsin B facilitate invasion of MCF-10A neoT cells through reconstituted matrix *in vitro*. *Exp Cell Res* **283**, 206–214.
7 Turk V, Turk B & Turk D (2001) Lysosomal cysteine proteases: facts and opurtunities. *EMBO J* **20**, 4629–4633.
8 Honey K & Rudensky AY (2003) Lysosomal cysteine proteases regulate antigen presentation. *Nat Rev Immunol* **3**, 472–482.
9 Turk B, Turk D & Salvesen GS (2002) Regulating cysteine protease activity: essential role of protease inhibitors as guardians and regulators. *Curr Pharm Dis* **8**, 1623–1637.
10 Brigger I, Dubernet C & Couvereur P (2002) Nanoparticles in cancer therapy and diagnosis. *Adv Drug Deliv Rev* **54**, 631–651.
11 Duncan R (1999) Polymer conjugates for tumour targeting and intracytoplasmic delivery. The EPR effect as a common gateway? *Pharm Sci Technol Today* **2**, 441–449.
12 Dinauer B, Balthasar S, Weber C, Kreuter J, Langer K & von Briesen H (2005) Selective targeting of antibody-conjugated nanoparticles to leukemic cells and primary T lymphocytes. *Biomaterials* **26**, 5898–5906.
13 Tokunaga E, Oki E, Nishida K, Koga T, Egashira A, Morita M, Kakeji Y & Maehara Y (2006) Trastuzumab and breast cancer: developments and current status. *Int J Clin Oncol* **11**, 199–208.
14 Nicolini A, Carpi A & Targo G (2006) Biomolecular markers of breast cancer. *Front Biosci* **11**, 1818–1843.
15 Kocbek P, Obermajer N, Cegnar M, Kos J & Kristl J (2007) Targeting cancer cells using PLGA nanoparticles surface modified with monoclonal antibody. *J Control Release* **120**, 18–26.
16 Cegnar M, Premzl A, Zavasnik-Bergant V, Kristl J & Kos J (2004) Poly(lactide-co-glycolide) nanoparticles as a carrier system for delivering cysteine protease inhibitor cystatin into tumour cells. *Exp Cell Res* **301**, 223–231.
17 Nielsen UB, Kirpotin DB, Piskering EM, Drummond DC & Marks JD (2006) A novel assay for monitoring internalization of nanocarrier coupled antibodies. *BMC Immunol* **7**, 24.
18 Brannon-Peppas L & Blanchette JO (2004) Nanoparticle and targeted systems for cancer therapy. *Adv Drug Deliv Rev* **56**, 1649–1659.

19 Plessers L, Bosmans E, Cox A, Beeck L, Vandepate J, Vanvuchelen J & Raus J (1990) Production and immunohistochemical reactivity of mouse antiepithelial monoclonal antibodies raised against human breast cancer cells. *Anticancer Res* **10**, 271–278.
20 Werner M, Wastelewski R, Bernhards J & Georga A (1990) Analysis of the tumour-associated antigen TAG 12 by monoclonal antibody 7A9 in normal, benign and malignant mammary tissues. *Virchows A Pathol Anat* **416**, 411–416.
21 Beketic-Oreskovic L, Sarcevic B, Malenica B & Novak DJ (1993) Immunocytochemical reactivity of a mouse monoclonal antibody CDI315B raised against human breast carcinoma. *Neoplasma* **40**, 69–74.
22 Kopitar-Jerala N, Bestagno M, Fan X, Novak-Despot D, Burrone O, Kos J, Skrk J & Gubensek F (2000) Molecular cloning and chimerisation of CDI 315B monoclonal antibody. *Eur J Physiol* **439**, 79–80.
23 Upasani OS, Vaidya MM & Bhisey AN (2004) Database on monoclonal antibodies to cytokeratins. *Oral Oncol* **40**, 236–256.
24 Osborn M (1987) Intermediate filament typing of cells and tumours yeilds information useful in histology and cytology. *Fortschritte Zool* **34**, 261–273.
25 Kasper M & Singh G (1995) Epithelial lung cell marker: current tools for cell typing. *Histol Histopathol* **10**, 155–169.
26 Kim RJ, Ro JY, Ahn SH, Kim HH, Kim SB & Gong G (2006) Clinicopathologic significance of the basal-like subtype of breast cancer: a comparison with hormone receptor and Her2/neu-overexpressing phenotypes. *Hum Pathol* **37**, 1217–1226.
27 Moll R (1994) Cytokeratins in the histological diagnosis of malignant tumours. *Int J Biol Markers* **9**, 63–69.
28 Nori A & Kopacek J (2004) Intracellular targeting of polymer-bound drugs for cancer chemoterapy. *Adv Drug Deliv Rev* **57**, 609–636.
29 Fonseca S, Simoes S & Gaspar R (2002) Paclitaxel-loaded nanoparticles: preparation, physicochemical characterisation and *in vitro* anti-tumoral activity. *J Control Release* **83**, 273–286.
30 Yin Win K & Feng SS (2005) Effects of particle size and surface coating on cellular uptake of polymeric nanoparticles for oral delivery of anticancer drugs. *Biomaterials* **26**, 2713–2722.
31 Obermajer N, Premzl A, Zavasnik-Bergant V, Turk B & Kos J (2006) Carboxypeptidase cathepsin X mediates β_2-integrin dependent adhesion of differentiated U-937 cells. *Exp Cell Res* **312**, 2515–2527.
32 Kos J, Dolinar M & Turk V (1992) Isolation and characterisation of chicken L- and H-kininogens and their interaction with chicken cysteine proteinases and papain. *Agents Actions Suppl* **28**, 331–339.
33 Holst-Hansen C, Johannessen B, Hoyer-Hansen G, Romer J, Ellis V & Brunner N (1996) Urokinase-type plasminogen activation in three human breast cancer cell liner with their *in vitro* invasiveness. *Clin Exp Metastasis* **14**, 297–307.